

1 **Tyre Wear Particles and Associated Chemical Pollutants:**

2 **Contribution to Urban PM_{2.5} in the Pearl River Delta**

3

4 Lele Tian^{1,4}, Shizhen Zhao^{*1}, Ruiling Zhang¹, Shaojun Lv¹, Duohong Chen², Jun Li¹, Kevin
5 C. Jones³, Ping'an Peng¹, Gan Zhang¹

6

7 ¹ State Key Laboratory of Organic Geochemistry and Guangdong Key Laboratory of
8 Environmental Resources Utilization and Protection, Guangzhou Institute of
9 Geochemistry, Chinese Academy of Sciences, Guangzhou 510640, China

10 ² State Environmental Protection Key Laboratory of Regional Air Quality Monitoring,
11 Guangdong Environmental Monitoring Center, Guangzhou 510308, China

12 ³ Lancaster Environment Centre, Lancaster University, Lancaster, LA1 4YQ, UK

13 ⁴ University of Chinese Academy of Sciences, Beijing 100049, China

14

15 *Corresponding author:

16 Shizhen Zhao

17 Email: zhaoshizhen@gig.ac.cn

18

19 **Abstract**

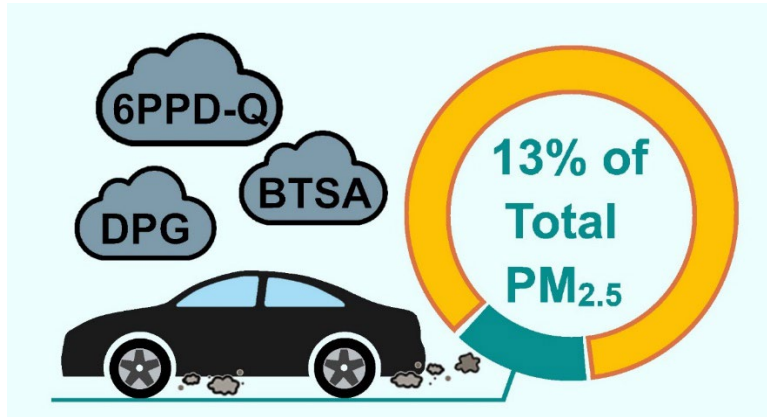
20 Tyre wear particles (TWPs) are a global concern due to their large emissions worldwide
21 and potential toxicity, as a vector for tyre wear chemicals (TWCs). However, the
22 contribution of TWPs to urban fine particles remains unknown. This study collected 72
23 paired gaseous and PM_{2.5} samples in urban air of the Pearl River Delta, China in 2018.
24 Among 54 targeted compounds, 28 TWCs ($\Sigma_{28}\text{TWCs}$) were detected. Total atmospheric
25 $\Sigma_{28}\text{TWCs}$ concentrations ranged from 3,130 to 317,000 pg/m³, mainly contributed in
26 the gaseous phase ($73 \pm 26\%$). Specifically, 2-OH-BTH ($82 \pm 21\%$) dominated in the gas
27 phase, while BTSA ($74 \pm 18\%$) dominated in PM_{2.5}. The cities of Guangzhou and Foshan
28 were identified as “hot spots” of TWCs. Most TWCs significantly correlated with nearby
29 road length. Measured gas-particle partition coefficients were higher than model
30 predictions, potentially caused by sampling artefacts, particulate burial and re-release
31 from TWPs itself. Importantly, source apportionment combined with characteristic
32 molecular indicators revealed that the TWPs contributed an average of $13 \pm 7\%$ to the
33 urban PM_{2.5}, highlighting their important contribution to urban air pollution and
34 potential threat to human exposure. These findings emphasize the urgent need for
35 initiatives aimed at reducing tyre wear emissions as part of broader strategies to
36 improve urban air quality.

37 **Keywords**

38 Tyre wear particles, gas-particle partition, fine particles, urban air, source
39 apportionment

40 **Synopsis**

41 Tyre wear particles (TWPs) make an important contribution to urban PM_{2.5} and the
42 load of gas-phase organic compounds in air, highlighting the urgent need for strategies
43 to reduce TWPs emissions.



46 Introduction

47 Tyre wear particles (TWPs) generated by the rolling shear of tread against a surface.¹
48 During the life of tyres, approximately 10-20% of their mass is released into the
49 environment through tyre wear.² It is estimated that global annual emissions of TWPs
50 more than 6 million tons, which means about 0.8 kg/capita/year.² TWPs was estimated
51 to contribute more than 50% to non-exhaust emissions (NEEs), which constituted 60%
52 of primary PM_{2.5} emissions from road transport.³⁻⁵ Several studies have found that
53 TWPs play a significant role in sources particles,^{3, 4, 6, 7} which is estimated that TWPs
54 accounted for 4-10% of PM_{2.5} emissions in tunnels⁴ and 12.3% in the roadway.⁸ The
55 contribution of TWPs is expected to continue growing and become the major source
56 of vehicular emission under various control measures mainly aimed at controlling
57 automobile exhaust emissions.⁹ However, the contribution of TWPs to urban
58 atmospheric PM_{2.5} is still unknown. Urban PM_{2.5} poses one of the greatest global
59 health risks,¹⁰ being associated with various negative health outcome such as lung
60 cancer,¹¹ cardiovascular disorders¹² and nervous system diseases.¹³

61 TWPs is also the carrier for tyre wear chemicals (TWCs), which are compounds referred
62 to as tyre additives and compounds emitted from tyre wear. These chemicals typically
63 including benzothiazoles (BTHs), p-phenylenediamines (PPDs), 1,3-diphenylguanidine
64 (DPG), hexa (methoxymethyl) melamine (HMMM) and benzotriazoles (BTRs). PPDs is
65 a “hotspot” of TWCs research due to their potential hazards to the environment and
66 human health. PPDs have widely reported in various environmental media, including
67 water, snow,¹⁴ air,^{15, 16} sediment¹⁷ and dust,¹⁸ even in human urine,¹⁹ human milk,²⁰
68 human serum²¹ and human cerebrospinal fluid.²² Among them, N-(1,3-dimethylbutyl)-
69 N'-phenyl-1,4-phenylenediamine-quinone (6PPD-Q), a quinone derivative of
70 antioxidant N-(1,3-dimethylbutyl)-N'-phenyl-p-phenylenediamine (6PPD) have the
71 acute mortality in salmon.²³ Moreover, PPDs and PPD-quinones, can induce oxidative
72 stress²⁴ and hepatotoxicity.^{25, 26}

73 Furthermore, certain TWCs, like 6PPD-Q, have demonstrated to be a promising
74 molecular indicator of TWPs,^{17, 27} indicating their potential utility in quantifying the
75 contribution of TWPs to atmospheric PM_{2.5} by source apportionment methods. It is
76 crucial to consider the environmental behavior of TWCs in urban atmosphere when
77 using them as organic molecular markers of TWPs.²⁸ Hence, it is of great importance

78 to investigate the gas-particle (G/P) partition affecting the environmental behavior of
79 TWCs. However, a comprehensive understating of their occurrence and fates
80 simultaneously in the gaseous and particulate phases of urban air is still lacking.

81 The Pearl River Delta (PRD) is an ideal region for studying TWPs and associated TWCs.
82 It is one of the four great Bay Areas in the world and has the largest vehicle inventory
83 in China.²⁹ It is also the center of China's new energy vehicle (NEV) industry
84 clustering.³⁰ The aims of this study were threefold: i) to investigate the occurrence and
85 atmospheric behavior, including gas-particle fractions, of typical TWCs in urban air of
86 the PRD region; ii) to quantify the contribution of TWPs to urban PM_{2.5} by characteristic
87 source indicators; and iii) to offer suggestion for reducing TWPs emissions. To our
88 knowledge, this study presents the first comprehensive dataset of TWCs in ambient air,
89 covering both gaseous and particulate phases. Our findings will provide valuable
90 insights into the environmental behavior of TWCs and important information to guide
91 the development of traffic control policies aimed at mitigating pollution in urban air.

92 **Materials and methods**

93 **Sampling Campaign**

94 The details of the sampling campaign were given in a previous study.³¹ Briefly, nine
95 prefecture-level cities of PRD, Shenzhen, Foshan, Dongguan, Zhongshan, Jiangmen,
96 Zhuhai, Zhaoqing, Huizhou and Guangzhou, were selected ([Table S1](#) and [Figure S1](#)). At
97 each site, gaseous and particulate (PM_{2.5}) phases pollutants were captured with
98 polyurethane foam plugs (PUFs, 14 cm in diameter × 7.5 cm in thickness, 0.02 g/cm³
99 in density) and quartz fibre filter (QFF, Whatman, 203 mm × 254 mm), respectively, by
100 high-volume active air sampler (Mingya Instruments Co., Guangzhou, China). The 24-
101 hour sampling was conducted continuously for 4 days in both winter (January to
102 February 2018) and summer (July to August 2018). Seventy-two paired gaseous and
103 PM_{2.5} samples were obtained in total. Before sampling, the QFFs were baked at 450 °C
104 overnight, and the PUFs were precleaned successively with acetone and
105 dichloromethane (DCM). All samples were delivered to the laboratory and stored at
106 -20 °C before analysis.

107 **Sample Pretreatment and Instrumental Analysis**

108 The chemicals and reagents information are given in [Text S1](#). After adding 50 ng D5-

109 6PPD-Q, d6-5-methylbenzotriazole (d6-5-MBTR), PPD-d10, BTR-D4 and 100 ng BTH-D4
110 as surrogate standards, QFFs and PUFs were ultrasonicated three times for 30 min with
111 methanol (MeOH). The extracts were evaporated to 0.5 mL and filtered with a 0.22
112 μm syringe filter. The filtrate was concentrated to 100 μL and spiked with 5 ng
113 benzophenone-d10 as internal standard before instrumental analysis.

114 Samples were analyzed by liquid chromatography and triple quadrupole mass
115 spectrometry (UPLC-MS/MS 8050, Shimadzu, Kyoto, Japan) on an instrument
116 equipped with an electrospray ionization source (ESI). Fifty-four compounds were
117 separated by a Waters X-Bridge BEH C18 column (2.1 mm \times 100 mm, 2.5 μm) with
118 three different mobile phases. Details of instrumental analysis were reported in our
119 previous studied^{32, 33} and described in [Text S2](#) and [Table S3 - S4](#).

120 The detailed sample treatment and instrumental analysis for water-soluble ions, trace
121 elements, organic carbon (OC), elemental carbon (EC) and polycyclic aromatic
122 hydrocarbons (PAHs) can be found in our previous studies^{34, 35} and described in [Text](#)
123 [S2](#).

124 **Quality Assurance and Quality Control (QA/QC)**

125 Solvent, field and procedural blanks were conducted to evaluate possible
126 contamination caused by solvent, sampling and pretreatment. Most compounds were
127 not detected or detected with a low contribution (<6%) in blanks, while benzothiazole
128 (BTH) and 3-cyclohexyl-1,1-dimethylurea (C-DMU) in blanks were detected accounting
129 for ~20% of their concentrations in samples, introduced by the nitrogen blowdown
130 step. The matrix recoveries ranged from 33 to 153% in PUFs and QFFs samples. The
131 average (\pm standard deviation) recoveries of pretreatment ranged from $51 \pm 1\%$ to 124
132 $\pm 2\%$, except for benzothiazole-2-sulfonic acid (BTSA, $288 \pm 89\%$) ([Table S5](#)). Further
133 experiments were conducted to justify the abnormally high recoveries of BTSA, as
134 detailed in [Text S3](#). Seven BTHs (2-mercaptobenzothiazole (2-SH-BTH), 2-
135 methylbenzothiazole (2-Me-BTH), 2-methylthio-benzothiazole (2-Me-S-BTH), 2-
136 chlorobenzothiazole (2-Cl-BTH), 2,5-dimethyl-1H-benzothiazole (XTH), 2-
137 (thiocyanomethylthio)benzothiazole (TCMTB) and BTH) were found to convert to BTSA.
138 Six recoveries (D5-6PPD-Q, d6-5-MBTR, PPD-d10, BTR-D4, and BTH-D4) ranged
139 between 55 - 129% in $\text{PM}_{2.5}$ samples and 62 - 141% in PUF samples. All reported
140 concentrations have been corrected by the blank and recoveries.

141 The calibration curve was made over 13 points (0.01–1000 µg/L) with all regression
142 coefficients higher than 0.99. The stability of LC-MS/MS was assessed by injecting two
143 concentrations (10 and 100 µg/L) of calibration standards between every 10 samples.
144 The instrumental detection limits (IDLs) and method detection limits (MDLs) were
145 0.001–20.5 ng and 0.098–503 pg/m³, respectively (Table S5).

146 **Backward Trajectories Simulation and PSCF model**

147 Backward particle release simulation and potential source contribution function (PSCF)
148 models have been widely used to identify the history of air masses and possible
149 geophysical pollution source locations, respectively.³¹ The PSCF analysis relied on the
150 results of backward trajectory calculated in our previous study using the Hybrid Single-
151 Particle Lagrangian Integrated Trajectory model (HYSPLIT 4.0,
152 <https://ready.arl.noaa.gov/HYSPLIT.php>). Briefly, 72 h backward trajectories were
153 computed at three-hour intervals and at a height of 500 m above ground level.³¹ More
154 details can be found in Text S4.

155 **Gas-particle Partitioning**

156 The G/P partition coefficient commonly describes the distribution of organic chemicals
157 between gaseous and particulate phases in the atmosphere.³⁶ Two widely used G/P
158 partition models, the Harner-Bidleman model³⁶ and the steady-state Li-Ma-Yang
159 model,^{37, 38} which use the octanol-air partition coefficients (K_{oa}), were employed to
160 predict the G/P partition quotients of TWCs, as detailed in Text S5. It should be noted
161 that only compounds with detection frequency > 30% in pairs of gaseous and
162 particulate phase samples were included.

163 **Positive Matrix Factorization (PMF)**

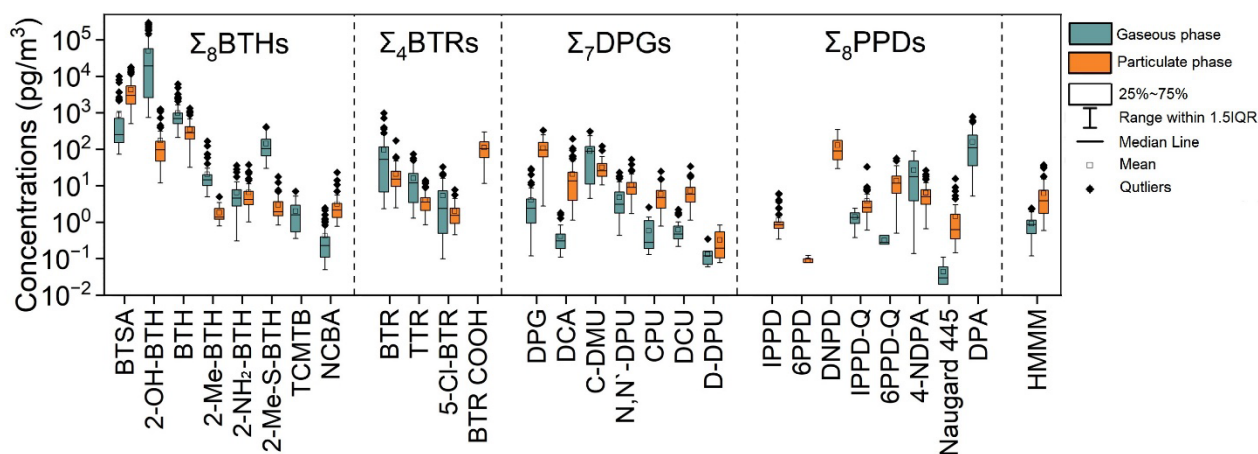
164 PMF is widely used to identify pollution sources and quantify contributions to ambient
165 air pollutants.³⁹ In this study, three TWCs (BTSA, DPG and 6PPD-Q) were identified as
166 tyre wear markers to quantify the contribution of TWPs. The screening step for tyre
167 wear markers and PMF analysis were detailed in Figure S2 and Text S6, respectively.

168 **Results and Discussion**

169 **Profile of TWCs in the Air of PRD**

170 Out of the 54 target analytes, 28 TWCs (Σ_{28} TWCs) were detected in total. Except for

171 BTSA and 2-OH-BTH, the remaining 26 chemicals are referred to as Σ_{26} TWCs. As
 172 detailed in [Text S7](#), the Σ_{26} TWCs were classified into five categories, Σ_6 BTHs, Σ_4 BTRs,
 173 Σ_7 DPGs, Σ_8 PPDs and HMMM, according to their chemical structure. The detection rate
 174 of Σ_{26} TWCs ranged between not detected (ND) and 100%, while the detection
 175 frequencies of 2-OH-BTH and BTSA were 97%-100% in both gaseous phases and PM_{2.5}.
 176 Overall, Σ_{28} TWCs concentrations ranged between 3,130 and 317,000 pg/m³, mainly in
 177 the gaseous phase (73 ± 26%). Σ_{28} TWCs concentrations in the gas and particulate
 178 phases were 587–312,000 pg/m³ and 375-18,500 pg/m³, respectively. Various
 179 composition patterns of TWCs were observed in the particulate and gas phases. The
 180 gas phase was dominated by 2-OH-BTH (82 ± 21%), whereas PM_{2.5} was dominated by
 181 BTSA (74 ± 18%). Specifically, 2-OH-BTH, Σ_6 BTHs and Σ_8 PPDs prevailed in the gas phase,
 182 accounting for 94 ± 17%, 75 ± 15% and 68 ± 33% for the total concentrations,
 183 respectively. BTSA, Σ_4 BTRs, Σ_7 DPGs and HMMM were more prevalent in PM_{2.5},
 184 contributing 80 ± 24%, 63 ± 32%, 69 ± 26% and 73 ± 25% to the total concentrations,
 185 respectively. The detection rates and concentrations of target compounds are detailed
 186 in [Table S6](#) and [Figure 1](#) and the pattern of Σ_{26} TWCs is shown in [Figure S3](#). Only the
 187 summed concentrations in the gas and PM_{2.5} phases are discussed further in this
 188 section.



189 Figure 1. The atmospheric profiles of Σ_8 BTHs (the sum of 2-OH-BTH, BTSA and Σ_6 BTHs),
 190 Σ_4 BTRs, Σ_7 DPGs, Σ_8 PPDs and HMMM from nine cities in PRD (n=72). IQR is the interquartile
 191 range. The green and orange box presented the concentration of gaseous and particulate
 192 phases, respectively.

193 Concentrations of BTSA ranged at 100-16,600 pg/m³ (median 3,170 pg/m³) in the PRD.
 194 Previous studies have reported that BTSA is an oxidative product of 2-SH-BTH.⁴⁰ We
 195 found it can also be transformed from the other six BTHs, except for 2-SH-BTH.

196 Although the exact formation pathway of BTSA is unclear, according to their chemical
197 structure (Figure S4), we speculate that sulfur dioxide (SO₂) may enhance the
198 production of BTSA, as SO₂ and SO₄²⁻ positively correlated with the BTSA level in PM_{2.5}
199 (Spearman, r=0.508-0.572, p<0.001). This finding also matched with the high particle-
200 bound fractions of BTSA (80 ± 24%).

201 Concentrations of 2-OH-BTH measured in this study ranged from 22.6 to 298,000
202 pg/m³ (median 17,800 pg/m³). Significantly, there is a pronounced seasonal difference
203 (Kruskal–Wallis H Test, p < 0.001), with a median concentration in summer (57,900
204 pg/m³) approximately 20 times higher than that in winter (2,730 pg/m³). It has been
205 proven that 2-OH-BTH is a product of BTH.⁴¹ A positive correlation was observed
206 between the ratio of 2-OH-BTH/BTH and temperature (Spearman, r=0.633, p<0.001),
207 suggesting that higher temperature promote the conversion of BTH to 2-OH-BTH in
208 summer.⁴²

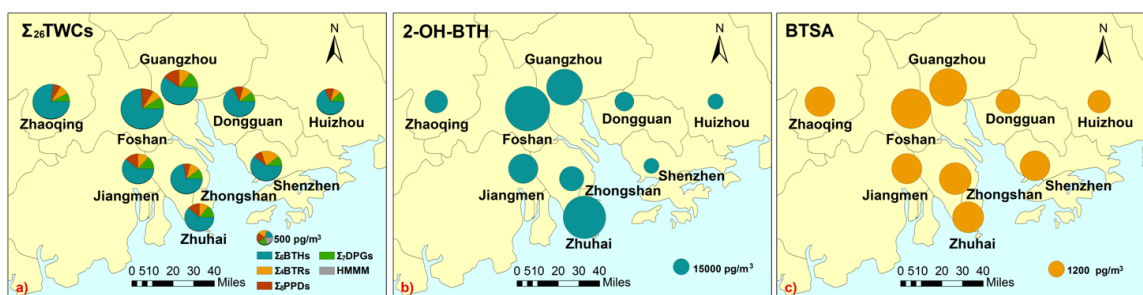
209 The Σ₂₆TWCs concentrations ranged between 956-8,300 pg/m³ (median 1,830 pg/m³)
210 with a significant seasonality (median 2,320 pg/m³ in summer vs 1,340 pg/m³ in winter,
211 Kruskal–Wallis H Test, p<0.001). Most TWCs concentrations were positively related to
212 temperature (Spearman, r=0.470-0.819, p<0.001), suggesting higher temperatures in
213 summer increase tyre wear rate, leading to more TWCs entering the environment.⁴³
214 As can be seen in Figure S3, Σ₂₆TWCs was dominated by Σ₆BTHs accounting for 38-86%
215 (65 ± 10%) and followed by Σ₇DPGs (12 ± 4%), Σ₄BTRs (11 ± 5%) and Σ₈PPDs (11 ± 7%).
216 The concentrations for most compounds were strongly correlated (Table S7),
217 consistent with them having similar sources.

218 DPG is used as a catalyst in tyre production to accelerate the cross-linking of rubber
219 materials with sulfur.⁴⁴ The German Environment Agency has identified DPG as a
220 potential persistent, mobile, and toxic (PMT) substance and very persistent and very
221 mobile (vPvM) substance,⁴⁵ indicating that DPG could pose environmental and human
222 health risks. The concentration of DPG varied from 3.45 to 300 pg/m³ (median 91.9
223 pg/m³), with a significant seasonal difference (Kruskal–Wallis H test, p=0.002). DPG has
224 been frequently detected at high concentrations in various environmental media such
225 as human urine, water and dust,⁴⁶⁻⁴⁸ which is attracting attention. However, there is
226 only one report of DPG in ambient air at a global scale from a passive sampler study.⁴⁹

227 6PPD-Q and N-isopropyl-N'-phenyl-1,4-phenylenediamine-quinone (IPPD-Q) are

228 ozonation products of 6PPD and N-isopropyl-N'-phenyl-1,4-phenylenediamine (IPPD),
 229 respectively. In this study, the level of 6PPD-Q ranged from ND to 50.5 pg/m^3 with a
 230 seasonal variation (Kruskal–Wallis H test, $p < 0.001$). Concentrations in winter (median
 231 $13.5 \text{ pg}/\text{m}^3$) were higher than in summer (median $8.16 \text{ pg}/\text{m}^3$). The concentration of
 232 IPPD-Q varied between ND– $31.1 \text{ pg}/\text{m}^3$ (median $1.84 \text{ pg}/\text{m}^3$). The detection frequency
 233 of IPPD-Q was 100% in winter, while only 31% in summer.

234 *Spatial Distribution*



235 Figure 2. The spatial distributions of $\Sigma_{26}\text{TWCs}$, 2-OH-BTH and BTSA in nine cities of the PRD,
 236 presented as average summed concentration of gaseous and particulate phases (pg/m^3)
 237 including winter and summer. This figure was modified from outputs of ArcGIS 10.4.1
 238 software, and the base map of China was from <http://www.arcgisonline.cn>.

239 Figure 2 presents the spatial distribution of $\Sigma_{26}\text{TWCs}$, 2-OH-BTH and BTSA, showing
 240 varied patterns in the PRD. The “hotspot” of $\Sigma_{26}\text{TWCs}$, 2-OH-BTH and BTSA was
 241 identified as Guangzhou ($2,630 \pm 782 \text{ pg}/\text{m}^3$, $71,900 \pm 52,100 \text{ pg}/\text{m}^3$ and $6,580 \pm 5,220$
 242 pg/m^3 , respectively) and Foshan ($3,540 \pm 2,490 \text{ pg}/\text{m}^3$, $110,000 \pm 128,000 \text{ pg}/\text{m}^3$ and
 243 $7,440 \pm 6,220 \text{ pg}/\text{m}^3$, respectively). As depicted in Figure 2, $\Sigma_6\text{BTHs}$ emerged as the
 244 most abundant compound among the $\Sigma_{26}\text{TWCs}$, with 2-OH-BTH and BTSA also
 245 belonging to BTHs. Notably, BTHs not only serve as tyre additives but also act as
 246 essential precursors for certain pharmaceuticals.⁵⁰ Moreover, high concentrations of
 247 BTHs and BTRs have been found in textiles.⁵¹ Considering Guangzhou and Foshan are
 248 important manufacturing centers for medicine and clothing in China,⁵² these industries
 249 may contribute significantly to the presence of BTHs in the PRD. Additionally, the
 250 sampling point in Guangzhou was located approximately 300 meters from a major
 251 express intersection, where vehicles frequently brake and decelerate when passing
 252 through the high-speed toll station, generating a large number of TWPs associated
 253 with increased concentration of TWCs. Notably, the concentration of 2-OH-BTH
 254 ($101,000 \pm 121,000 \text{ pg}/\text{m}^3$) was second highest in Zhuhai, which may be associated

255 with a point source near the sampling site. Within one kilometer of sampling point in
256 Zhuhai, three driving schools, one karting club, and four high-speed toll stations were
257 identified, all potentially contributing significant amount of TWPs.

258 ***Comparison with Other Studies***

259 The comparison of gas and particulate phase concentration with literature is detailed
260 in [Table S8](#). Only two studies have reported the occurrence of four BTHs⁵³ and five
261 BTRs⁵⁴ in indoor gaseous phase. Compared with indoor air,⁵³ the BTHs concentrations
262 in the urban atmosphere gas phase show different profiles. The median gas phase
263 concentration of BTH in urban air was 700 pg/m³, which was 20 times lower than
264 observed in indoor air (14,200 pg/m³). Conversely, 2-OH-BTH measured in urban
265 atmospheric gaseous phase was 17,700 pg/m³, which was 20 times higher than that
266 in indoor air (860 pg/m³). One explanation could be that higher temperatures and
267 stronger UV radiation outdoors favor the degradation of BTH into 2-OH-BTH.^{40, 41} For
268 BTRs, our median level in urban gaseous phase, ranging from 2.34 pg/m³ to 53.3 pg/m³,
269 was 10 to 35 times higher than that in indoor air.⁵⁴ BTRs are widely used to inhibit the
270 corrosion of metal alloys in vehicles or are added to aircraft de-icing agents and fluids,
271 making them more prevalent outdoors than indoors.³²

272 As illustrated in [Figure S7](#), the levels of 2-OH-BTH in this study exhibit a broader range
273 (ND-1,130 pg/m³) with a lower median concentration (84.4 pg/m³) compared to
274 previous reports in Taiyuan, Shanghai, and Guangzhou (range 66.8-557 pg/m³ with
275 median 152-455 pg/m³) in PM_{2.5}.⁴² This variation could be attributed to the point
276 sources near the sampling points in Guangzhou and Zhuhai, as mentioned earlier. Our
277 BTH concentrations (median 256 pg/m³) were an order of magnitude higher than that
278 in Taiyuan, Shanghai, and Guangzhou (median 32.6-55.9 pg/m³) in PM_{2.5}.⁴² In contrast,
279 the levels of 2-Me-S-BTH and 2-aminobenzothiazole (2-NH₂-BTH) in PM_{2.5} (median
280 1.52 and 3.65 pg/m³) were an order of magnitude lower than those reported in other
281 studies.^{42, 55} Overall, the concentration of BTHs in our study is notably higher than
282 reported in previous literature.

283 DPG and HMMM in the atmosphere were only reported on the global scale by passive
284 sampling.⁴⁹ The global median level of DPG was comparable to our study (93.9 pg/m³
285 vs 91.9 pg/m³), while the HMMM concentration was considerably lower in the global
286 survey (0.11–0.22 pg/m³ vs 0.65–34.4 pg/m³) than our observations.⁴⁹ Different from

287 other studies, N-(1,4-dimethylpentyl)-N'-phenylbenzene-1,4-diamine (7PPD), N-(1,4-
288 dimethylpentyl)-N-phenylbenzene-1,4-diamine (77PD), N,N'-diphenyl-p-
289 phenylenediamine (DPPD), N,N'-di-(p-tolyl)-phenylenediamine (DTPD), N-phenyl-N'
290 -cyclohexyl-p-phenylenediamine (CPPD), 77PD-quinone (77PD-Q), DPPD-quinone
291 (DPPD-Q) and CPPD-quinone (CPPD-Q) were not detected in this study.^{15, 16, 18, 24, 56}
292 Additionally, the detected IPPD and IPPD-Q in PM_{2.5} were present at lower
293 concentrations (median 0.74 pg/m³ and 1.64 pg/m³ for IPPD and IPPD-Q, respectively)
294 than those reported in Guangzhou, Taiyuan, Zhengzhou, Shanghai, Nanjing and
295 Hangzhou (median 1.1-230 pg/m³ and 2.00-65.5 pg/m³ for IPPD and IPPD-Q,
296 respectively).^{15, 16, 18, 24} Additionally, compared with literature (median 1.18-25.5 pg/m³),
297 ^{16, 18, 24} the 6PPD-Q level was at a median range in this study (median 10.4 pg/m³).

298 **Influencing Factors**

299 **Socio-economic Parameters**

300 The concentration of most TWCs shows a significant correlation with road length
301 within a two-kilometer radius of the sampling sites (Spearman, $r=0.242-0.525$,
302 $p<0.001-0.041$) and the production volume of rubber tyres in the PRD (Spearman,
303 $r=0.542-0.773$, $p<0.001-0.021$), as detailed in [Table S9](#). This suggests that TWCs are not
304 solely emitted by TWPs but are also released during tyre production processes.
305 Additionally, it is noteworthy that the level of most BTHs were positively related to the
306 length of dyed fabrics (Spearman, $r=0.369-0.495$, $p<0.001-0.002$), implying potential
307 sources of BTHs in textiles.⁵¹

308 Interestingly, the concentration of HMMM was positively correlated with human
309 activities, including the residential land area within a one/two/five/ten/twenty-
310 kilometer radius of the sampling sites, permanent population density and automobile
311 population (Spearman, $r=0.269-0.389$, $p=0.001-0.028$). HMMM, added to tyres as an
312 organic vulcanizer to enhance durability and strength,⁵⁷ has been widely detected in
313 various environmental media.^{49, 58} The observed positive correlation of HMMM levels
314 with human activities, coupled with its widespread detection in various environmental
315 media, suggests that HMMM may serve as a suitable indicator for assessing human
316 activity.

317 **Meteorological Parameters**

318 A significantly negative correlation was found between the concentrations of most

319 directly emitted TWCs (e.g., 4-methyl-1H-benzotriazole and 5-methyl-1H-
320 benzotriazole, TTR) and PM_{2.5}. Conversely, a positive correlation was observed
321 between the concentrations of most product TWCs (e.g., 6PPD-Q) and PM_{2.5}. This
322 implies that the product TWCs achieved a co-benefit reduction with PM_{2.5}.

323 Furthermore, the concentrations of most TWCs exhibited a positive correlation with
324 relative humidity (RH) (Spearman, $r=0.327-0.794$, $p<0.001-0.007$), while
325 demonstrating a negative correlation with wind speed (Spearman, $r=-0.308\sim-0.605$,
326 $p<0.001-0.037$). This suggests that higher RH and lower wind speeds are
327 disadvantageous for pollution diffusion,⁵⁹ resulting in elevated concentrations of TWCs
328 in the atmosphere.

329 **The Influence of Monsoons**

330 To comprehend the influence of monsoons and regional sources on TWCs, PSCF model
331 results and 24 h distribution of air mass concentrations was drawn and presented in
332 [Figure S5](#). During the sampling period, summer air masses were predominantly from
333 the South China Sea. Winter air masses mainly originated from the East China Sea and
334 South China Sea in Guangzhou, while from northern inland regions in other sites.

335 The PSCF results ([Figure S5-S6](#)) indicated that only the TWCs of Guangzhou during
336 summer were influenced by air masses from the South China Sea, while other sites
337 were primarily affected by local sources in both winter and summer. As TWCs are
338 compounds associated with tyre wear, they may enter the environment via TWPs.
339 Numerous studies have demonstrated that the ocean is an important sink for MPs,
340 which included TWPs.⁶⁰⁻⁶² Tyre dust contributes 34% to the amounts entering the
341 aquatic environment in mainland China in 2015.⁶⁰ However, recent studies suggest
342 that TWPs in the ocean may be re-emitted into the marine atmosphere through sea
343 spray and bubble bursting, transforming the ocean from a sink into an important
344 source of atmospheric TWPs.⁶¹ The South China Sea is one of the most polluted areas
345 of MPs in China.⁶² Therefore, the summer monsoon may carry TWCs from marine
346 atmosphere of South China Sea into Guangzhou. The percentage difference of Σ_{28} TWCs
347 concentration between winter and summer in Guangzhou was the smallest among all
348 sampling sites (1.03 vs 1.20-1.83), which could be attributed to the marine source by
349 summer monsoon in Guangzhou.

350 Gas-particle Fractions

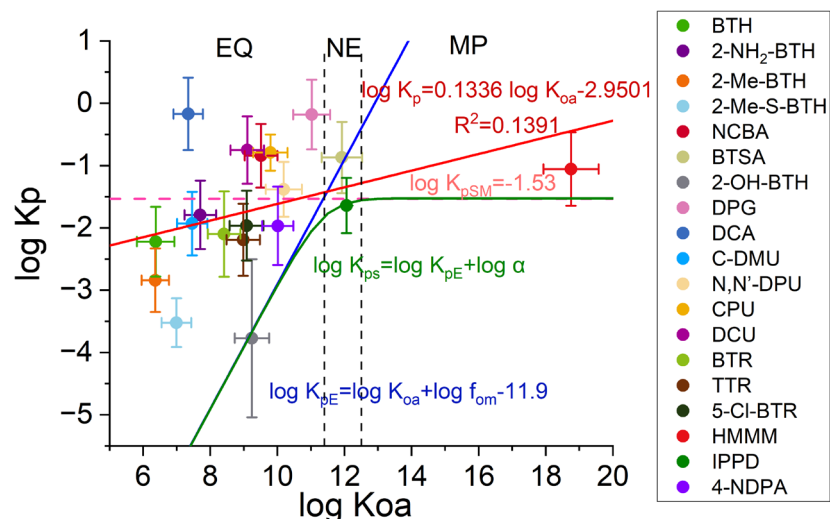
351 The gas-particle fraction largely varied among TWCs in this study (Figure S8). The
352 particle-bound partition of BTHs ranged from 2-Me-S-BTH at $2 \pm 2\%$ to BTSA at $80 \pm$
353 24% , DPGs ranged from C-DMU at $42 \pm 36\%$ to *N,N*-dicyclohexylmethylamine (DCA) at
354 $96 \pm 4\%$. BTRs varied from TTR at $23 \pm 24\%$ to BTR COOH 100% and PPDs ranged from
355 diphenylamine (DPA) at 0% to IPPD at $99 \pm 12\%$. HMMM played a dominant role in
356 particulate phase, accounting for $73 \pm 25\%$. Compared with indoors,^{53, 54} the G/P
357 partitioning of most BTHs and benzotriazole (BTR) compounds have a similar trend,
358 but 2-OH-BTH and TTR have a higher fraction in the particles in this study. Most BTHs
359 and BTRs, especially the dominant 2-OH-BTR and BTH, were primarily enriched in
360 gaseous phase, underscoring the significance of TWCs in gaseous phase for
361 environmental and human health impact.

362 The G/P partitioning is affected by various factors such as the sources of particles,
363 temperature and physicochemical properties.⁶³ As listed in Table S10, a significant
364 positive correlation was found between particle-bound fraction of most TWCs and
365 $PM_{2.5}$ concentrations (Spearman, $r=0.244-0.676$, $p<0.001-0.042$), which may indicate
366 the particle level would affect the particle-bound fraction. Additionally, particle-bound
367 partition of most TWCs and aerosol liquid water content (ALWC, detailed calculations
368 in Text S8) also showed a positive correlation (Spearman, $r=0.239-0.595$, $p<0.001-$
369 0.046), implying that an increased ALWC in particles leads to a greater number of
370 dissolved targets due to their hydrophilicity. Meanwhile, a strong negative correlation was
371 observed between temperature and particle-bound partition of most target
372 compounds (Spearman, $r=-0.247\sim-0.792$, $p<0.001-0.037$), suggesting that chemicals
373 are more prone to enter gaseous phase in higher temperature.⁶³

374 The most measured G/P coefficient ($\log K_p$) and $\log K_{oa}$ of TWCs were positively
375 associated (Spearman, $r=0.417-0.760$, $p<0.001$, Table S11), suggesting that the $\log K_p$
376 of TWCs could be predicted by $\log K_{oa}$.⁶⁴ Two widely used G/P partitioning models,
377 Harner-Bidleman model³⁶ and steady-state Li-Ma-Yang model,^{37, 38} were employed to
378 predict the G/P partition quotient of TWCs. The slopes of measured $\log K_p$ and $\log K_{oa}$
379 were below unity among TWCs, which implies nonequilibrium G/P partitioning of
380 targets. Two threshold $\log K_{oa}$ values ($\log K_{oa1}=11.4$ and $\log K_{oa2}=12.5$, detailed as Text
381 S5) divided partitioning map into three domains by steady-state Li-Ma-Yang model.⁶⁵

382 As depicted in [Figure 3](#), HMMM exhibited the highest log K_{oa} (>12.5) and the
383 measured log K_p was closer to the steady-state Li-Ma-Yang model, suggesting that the
384 steady-state model might offer a better fit for predicting the G/P fractions of HMMM.
385 In the non-equilibrium domain (NE, 11.4<log K_{oa}<12.5), measured log K_p of BTSA
386 worked well by Harner-Bidleman model, while measured log K_p of IPPD was well-fitted
387 by Li-Ma-Yang model. For compounds including HMMM, BTSA, IPPD, characterized by
388 higher log K_{oa} (>11.4), a closer fit between detected and predicted log K_p was
389 observed. This suggested that the particle fraction of these compounds might be
390 primarily driven by K_{oa} rather than molecular interactions between compounds and
391 particles.⁶⁶

392 Compared with measured log K_p, except for 2-OH-BTH, HMMM, BTSA and IPPD,
393 predicted log K_p by two models were underestimated in the equilibrium domain (EQ,
394 log K_{oa}<11.4) as depicted in [Figure 3](#). The underestimation of predicted log K_p may be
395 attributed to three possible reasons. Firstly, the QFFs may absorb gaseous chemicals
396 into particles, a sampling artifact, leading to an overestimation of their concentrations
397 in PM_{2.5}.⁶⁷ Secondly, for compounds with strong hydrophilicity, residing on the particle
398 surface for sufficient time may result in a portion of these compounds being “buried”
399 into PM_{2.5} and not readily diffuse back to the particle surface and into the gaseous
400 phase. This can lead to elevated levels of these substances in particles.^{68, 69} Lastly,
401 TWPs entering the atmosphere might become part of PM_{2.5} without releasing
402 additives, causing these additives to be “buried” into PM_{2.5} along with TWPs.
403 Conversely, the higher vapor pressure of 2-OH-BTH (4.4 Pa at 25 °C) makes it more
404 prone to volatilization from the tyre and PM_{2.5}. This explains why the predicted G/P
405 fraction of log K_p of 2-OH-BTH can be fitted by the model even with low log K_{oa}.
406 Furthermore, various hydrophilic substances, such as organophosphate flame
407 retardants (OPFRs),⁷⁰ were also found to underestimated log K_p by models, warranting
408 further investigation.



409

410 Figure 3. Log-log plots of K_p , K_{pE} , $\log K_{pS}$ and $\log K_{oa}$ for TWCs. $\log K_p$, the regression of
 411 measured $\log K_p$, was presented as red solid line. $\log K_{pE}$ (blue solid line) and $\log K_{pS}$ (green
 412 solid line) were calculated using Harner-Bidleman model and Li-Ma-Yang model,
 413 respectively. For $\log K_{oa}$, the left vertical black dashed line is the first $\log K_{oa}$ threshold (\log
 414 $K_{oa1} = 11.4$) dividing it into equilibrium domain (EQ) and non-equilibrium domain (NE), while
 415 the right vertical black dash is the second $\log K_{oa}$ threshold ($\log K_{oa2} = 12.5$) starting the
 416 maximum partitioning (MP) domain as detailed in Text S5. $\log K_{pSM} = -1.53$ (the horizontal pink
 417 dashed line) is the maximum constant value of calculated by steady-state Li-Ma-Yang
 418 model.³⁷

419 Contribution of TWP to PM_{2.5}

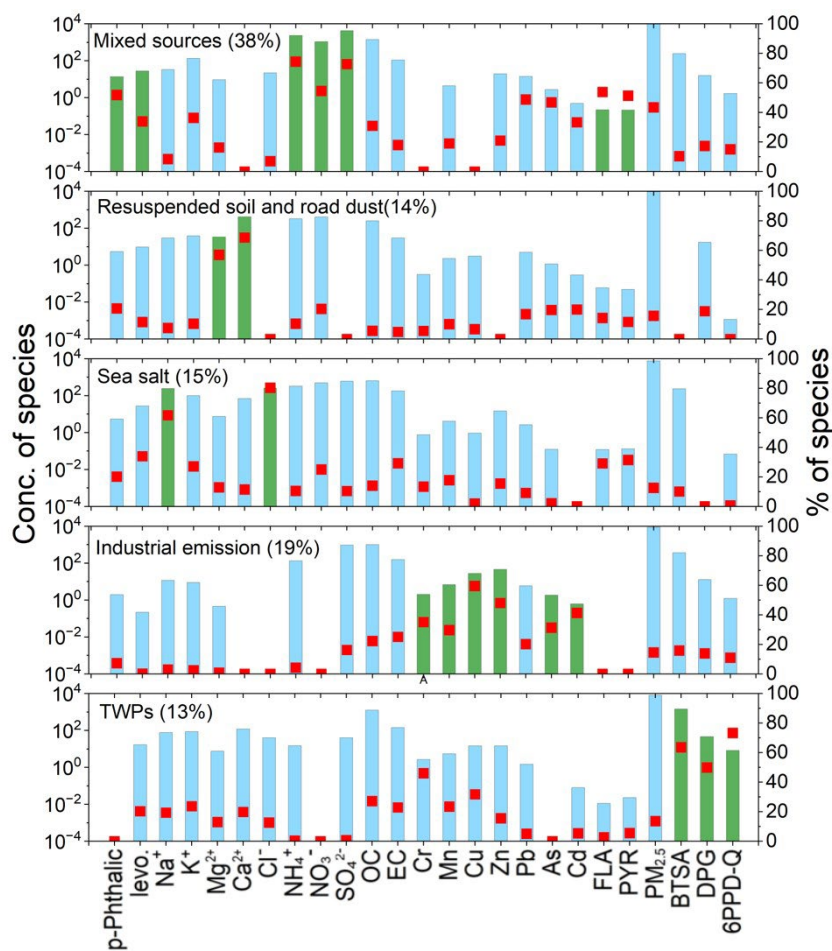
420 In this study, TWCs were used as markers of TWPs to more accurately quantify the
 421 contribution of TWPs to PM_{2.5} by PMF. The utilization of TWCs in the PMF analysis
 422 followed four essential criteria, as illustrated in Figure S2. Briefly, firstly, TWCs were
 423 widely detected (detection rate >80%) in this study. Secondly, TWCs were primarily
 424 enriched in PM_{2.5} (with their concentration in PM_{2.5} exceeding 50% of the total gaseous
 425 and particle phases concentrations), as indicated by the results of G/P partitioning.
 426 This suggests that TWCs are closely linked to PM_{2.5} and exhibit limited partitioning into
 427 the gas phase. Thirdly, TWPs were identified as unique sources of TWCs. Lastly, the
 428 correlation coefficient (r^2) exceeded 0.7, and factor profile results were interpretable
 429 in PMF results. Subsequently, three TWCs (BTSA, DPG and 6PPD-Q) were finally
 430 identified. In PMF analysis, three-eight factors were performed in PMF model and five
 431 factors were determined as the optimal number of sources based on considerations of
 432 Q/Qexp value, repeatability and model interpretability (Figure S9). The specific details
 433 of PMF analysis and factor profile are provided in Text S6 and Figure 4, respectively.

434 The first factor, characterized by high fractions of p-phthalic acid, levoglucosan (levo.),
435 K^+ , NH_4^+ , NO_3^- , SO_4^{2-} , fluoranthene (FLA) and pyrene (PYR), is identified as a mixed
436 source associated with secondary formation, vehicle exhaust, biomass burning and
437 plastic waste combustion. Specifically, p-phthalic acids are indicators of plastic
438 burning.⁷¹ Levo. and K^+ are acknowledged markers indicative of biomass burning.^{72, 73}
439 The presence of NH_4^+ , NO_3^- and SO_4^{2-} is associated with secondary aerosols.⁷⁴ FLA and
440 PYR have a high level in motor vehicle exhaust.⁷⁵ Moreover, vehicle exhaust and
441 biomass burning are recognized as important contributors to secondary formation of
442 NO_x and SO_4 .⁷⁶ This mixed source had the highest contribution to $PM_{2.5}$ at $38 \pm 7\%$.

443 The second factor was dominated by Mg^{2+} and Ca^{2+} , which are typical tracers of
444 resuspended soil and road dust.^{77, 78} It is higher in winter ($17 \pm 8\%$) than summer (11
445 $\pm 6\%$) with seasonal variation (Kruskal–Wallis H test, $p=0.005$). Previous studies found
446 that RH and wind speed significantly influence the generation and resuspension of
447 dust.⁷⁸ The contribution of soil and road dust was negatively correlated with RH
448 (Spearman, $r=-0.604$, $p<0.001$), while positively correlated with wind speed (Spearman,
449 $r=0.378$, $p=0.008$) in this study. These correlations support to the reasonableness of
450 PMF results.

451 The third factor was characterized by Na^+ and Cl^- , representing the source of sea salt.⁷⁹
452 Its contribution was slightly higher in winter ($14 \pm 5\%$) than summer ($16 \pm 13\%$) with
453 seasonality (Kruskal–Wallis H test, $p=0.018$). The summer monsoon (Figure S5) could
454 carry the sea salt from the coastal region into the PRD, resulting in the seasonality.

455 The fourth factor was attributed to industrial emissions, primarily from metals such as
 456 Cu, Zn, Cr, Mn, Cd, and As, which exhibited substantial loading (19%). Industrial
 457 emissions, particularly from iron and steel industries as well as non-ferrous industries,
 458 emerged as the predominant sources of these metals.⁸⁰ Industrial emissions
 459 contributed $19 \pm 7\%$ to PM_{2.5} in the PRD.



460 Figure 4. Source profiles gained from PMF analysis of PM_{2.5}. Bars represent concentration of
 461 selected species and red squares represent contribution (%) of selected specie.

462 The fifth factor shows a high loading of BTSA, DPG and 6PPD-Q, which are identified
 463 as TWPs. BTSA, DPG and 6PPD-Q serve as tracers of TWPs in this study (detailed in
 464 [Figure S2](#)). Recent studies have proposed 6PPD-Q as a promising marker for tyre
 465 wear.^{17, 27} Additionally, BTSA is set as the total variable in the PMF model to quantify
 466 its source composition, as the details of [Text S6](#) and [Figure S10](#). The results showed
 467 that the contribution of TWPs to BTSA is $55 \pm 17\%$, which indicates that TWPs are the
 468 main source of BTSA. This suggests the rationality of BTSA as TWPs indicator. The
 469 contribution of TWPs to PM_{2.5} ranged from 6% (Zhaoqing) to 25% (Guangzhou) without

470 seasonality (Figure S11). As shown in Figure S12, Guangzhou, where sampling near the
471 highway intersection toll station, showed the highest contribution of TWPs at 25% to
472 PM_{2.5}.

473 It's noteworthy that previous studies have reported several organic compounds as tyre
474 wear markers, such as N-cyclohexyl-1,3-benzothiazol-2-amine (NCBA) and 2-(4-
475 Morpholinyl) benzothiazole (24MoBT).⁸¹ However, in this study, these markers
476 exhibited low detection frequencies, with 24MoBT not being detected in all samples.
477 This could be attributed to the change of predominant vulcanization accelerator of tyre
478 rubber,⁸² suggesting that they may no longer suitable as molecular markers of tyre
479 wear.

480 Previous studies have assessed the contribution of tyre wear by metal markers such as
481 Zn, Mn and Cu. For instance, Zhang *et al.* reported that tyre wear contributed 4 ± 2 %
482 to PM_{2.5} in Beijing, Tianjin, Zhengzhou and Qingdao based on tunnel measurements.⁴
483 Similarly, tyre wear in road air contribute 6.6% to fine particles in Tianjin,³ 5.2 % to
484 PM_{2.5} in Shanghai⁶ and 10.7 ± 2.3 % to PM_{0.9-11.5}.⁷ However, it is important to note that
485 metals do not only solely originate from tyre wear but are also emitted by activities
486 such as coal combustion, steel industry, metallurgy.⁸³ Consequently, the complexity of
487 metal sources may lead to larger uncertainty in quantifying the contribution of TWPs
488 to fine particles. In our study, the contribution of TWPs to PM_{2.5} and the road length
489 within a five-kilometer radius of the sampling sites was positively correlated ($r^2=0.67$)
490 as in Figure S13. This supports the rationality of using BTSA, DPG and 6PPD-Q as
491 markers to quantify the contribution of TWPs to PM_{2.5}.

492 **Limitations and Environmental Implications**

493 In this study, the concentrations of 77PD, DTPD, DNP, 6PPD and DPPD decreased in
494 MeOH solvent ranging from 17% (6PPD) to 100% (77PD) during a 132-hour chemical
495 stability test (Table S11). Although a significant decline in the concentrations of PPDs,
496 no noticeable increase observed in the concentration of PPDQs. Moreover, in our
497 previous study,³² the levels of 6PPD, DPPD, IPPD, DNP, CPPD and 77PD in a MeOH:
498 water solvent mixture (1:9 ,v/v) decreased by 42% (IPPD) to 100% (77PD) in three days.
499 This suggests increased instability of PPDs when exposed to aqueous conditions.²³ As
500 a result, the instability of PPDs could be responsible for the low detection rate in air
501 samples and their underestimated measured level in air. During field work, it is

502 challenging to pretreat and analyze samples immediately. Despite this, field
503 observations still serve as a valuable reference for understanding their occurrence and
504 fates in the environment.

505 Our study is the first to report ultra-high concentrations of BTSA (ranged at 0.1-166
506 ng/m³, median 3.17 ng/m³) with 100 % detection frequency in the atmosphere.
507 Although seven BTHs may convert to BTSA during pretreatment, the converted BTSA
508 only accounted for 2.19 ± 3.07% (median 1.52%) of the total BTSA concentration (Text
509 S3), which can be considered negligible. To our knowledge, BTSA has been reported as
510 a transformation product of 2-SH-BTH, without record of its direct use. Previous
511 research observed that BTSA was dominant (332 µg/g) in extracted solution of tyre
512 and road wear particles (TRWPs), whereas only 74.8 µg/g was found in the cryo-milled
513 tire tread (CMTT) extraction. However, the content of extractables in TRWP was higher
514 than that in CMTT by five-eight-fold.⁸⁴ The disparity in the composition of BTSA
515 between TRWP and CMTT implies that tire wear is a significant process in BTSA
516 formation. So far, the transformation pathway, environmental behavior and potential
517 biological toxicity of BTSA are rarely studied, thus further research is urgently needed.

518 China has implemented various control measures, including improvement in exhaust
519 emissions and fuel standards, as well as encouraging the development of NEV, to
520 control automobile exhaust pollution.⁹ As a result, the contribution of motor vehicle
521 exhaust emissions (VEE) has decreased, while the contribution of NEE has increased
522 with the rise in car ownership. In UK, particles emitted by NEE contribute 60% to
523 primary PM_{2.5} emissions from road transport and constitute 7.4% of all UK primary
524 PM_{2.5}.⁵ This suggested that NEEs have become a dominant source of traffic pollution
525 in UK. We attempted to parse VEE source as independent factors when conducting
526 source apportionment by PMF model. Unfortunately, VEE could not be separated from
527 secondary nitrates in this study. Alternatively, the contribution of VEE to PM_{2.5} from
528 the PRD in the literature is used to compare with the contribution of TWPs to PM_{2.5}.^{85,}
529 ⁸⁶ In our study, TWPs account for 13 ± 7% of PM_{2.5} in PRD, comparable with VEE (13%
530 - 14%) of PM_{2.5} in the PRD region.^{85,86} However, it can be seen that the contribution of
531 TWPs will keep growing, owing to the phasing-out of fossil-fueled cars and the
532 increasing popularity of NEVs. Besides, NEVs, having relatively high weight,
533 accelerating the particle emissions of TWPs.⁸⁷

534 China, being the largest consumption market for NEVs, has witnessed a significant

535 increase in NEV sales, with annual growth rates 166% from 2011 to 2022.⁸⁸ In 2020,
536 China's automobile sales volume was 25.31 million of which 1.37 million were NEV,
537 accounting for 5.4% of automobile sales.⁸⁸ In 2035, NEVs are expected to achieve a
538 market share of 50% and become the mainstream.⁸⁹ Additionally, to 2050 if the world
539 avoids the worst global climate change scenarios, globally new vehicles will be almost
540 entirely electric vehicles.⁸⁹ The rapid development of NEVs implies that NEEs will
541 become a major contributor to traffic pollution in the near future. Currently, there is
542 no released legislation, restrictions to control/reduce NEEs in any country and region
543 of the world. Reducing NEE to minimize environmental pollution can be approached
544 from three aspects: regulations, technology, and management. On one hand, efforts
545 should be made to enhance the development of technologies such as reducing the
546 weight of NEE, accompanied by the supporting facilities of NEE treatment for vehicles,
547 such as the Tyre Collective developed by a clean-tech company in the UK,
548 (<http://thetyrecollective.com>). On the other hand, the government should optimize
549 road-related policies, and regulations regarding NEE. Simultaneously, road
550 management should be optimized to reduce traffic congestion, as it plays a crucial role
551 in minimizing NEE.

552 **Acknowledgement**

553 This work is supported by the Guangdong Major Project of Basic and Applied Basic
554 Research (2023B0303000007), National Natural Science Foundation of China (Nos.
555 42107120), the Alliance of International Science Organizations (Grant No. ANSO-CR-
556 KP-2021-05), Guangdong Basic and Applied Basic Research Foundation
557 (2023B1515020067 and 2023B1212060049), Youth Innovation Promotion Association
558 of CAS (2022359), and Tuguangchi Award for Excellent Young Scholar GIG (TGC202204).
559 Many thanks to the volunteers involved in the field work.

560 **References**

561 1. Rogge, W. F.; Hildemann, L. M.; Mazurek, M. A.; Cass, G. R.; Simoneit, B. R. T.,
562 SOURCES OF FINE ORGANIC AEROSOL .3. ROAD DUST, TIRE DEBRIS, AND
563 ORGANOMETALLIC BRAKE LINING DUST - ROADS AS SOURCES AND SINKS.
564 *Environmental Science & Technology* **1993**, *27*, (9), 1892-1904.

- 565 2. Kole, P. J.; Lohr, A. J.; Van Belleghem, F. G. A. J.; Ragas, A. M. J., Wear and Tear of
566 Tyres: A Stealthy Source of Microplastics in the Environment. *International Journal of*
567 *Environmental Research and Public Health* **2017**, *14*, (10).
- 568 3. Zhang, Q. J.; Liu, J. Y.; Wei, N.; Song, C. B.; Peng, J. F.; Wu, L.; Mao, H. J., Identify the
569 contribution of vehicle non-exhaust emissions: a single particle aerosol mass
570 spectrometer test case at typical road environment. *Frontiers of Environmental Science*
571 *& Engineering* **2023**, *17*, (5).
- 572 4. Zhang, J.; Peng, J.; Song, C.; Ma, C.; Men, Z.; Wu, J.; Wu, L.; Wang, T.; Zhang, X.; Tao,
573 S.; Gao, S.; Hopke, P. K.; Mao, H., Vehicular non-exhaust particulate emissions in
574 Chinese megacities: Source profiles, real-world emission factors, and inventories.
575 *Environmental Pollution* **2020**, *266*.
- 576 5. Non-exhaust emissions from road traffic. In Department for Environment, F. a. R. A.;
577 Government, S. G. W.; Ireland, D. o. t. E. i. N., Eds. Air Quality Expert Group,
578 Department for Environment Food and Rural Affairs: London, 2019.
- 579 6. Wang, Q. Q.; Qiao, L. P.; Zhou, M.; Zhu, S. H.; Griffith, S.; Li, L.; Yu, J. Z., Source
580 Apportionment of PM_{2.5} Using Hourly Measurements of Elemental Tracers and Major
581 Constituents in an Urban Environment: Investigation of Time-Resolution Influence.
582 *Journal of Geophysical Research-Atmospheres* **2018**, *123*, (10), 5284-5300.
- 583 7. Harrison, R. M.; Jones, A. M.; Gietl, J.; Yin, J. X.; Green, D. C., Estimation of the
584 Contributions of Brake Dust, Tire Wear, and Resuspension to Nonexhaust Traffic
585 Particles Derived from Atmospheric Measurements. *Environ. Sci. Technol.* **2012**, *46*,
586 (12), 6523-6529.
- 587 8. Matthaios, V. N.; Lawrence, J.; Martins, M. A. G.; Ferguson, S. T.; Wolfson, J. M.;
588 Harrison, R. M.; Koutrakis, P., Quantifying factors affecting contributions of roadway
589 exhaust and non-exhaust emissions to ambient PM_{10-2.5} and
590 PM_{2.5-0.2} particles. *Sci. Total Environ.* **2022**, *835*.
- 591 9. Zhang, X.; Wang, Q. L.; Qin, W. N.; Guo, L. M., Sustainable Policy Evaluation of Vehicle
592 Exhaust Control-Empirical Data from China's Air Pollution Control. *Sustainability* **2020**,
593 *12*, (1).
- 594 10. Zhao, C. C.; Pan, J. H.; Zhang, L. L., Spatio-Temporal Patterns of Global Population
595 Exposure Risk of PM_{2.5} from 2000-2016. *Sustainability* **2021**, *13*, (13).
- 596 11. Han, X.; Liu, Y. Q.; Gao, H.; Ma, J. M.; Mao, X. X.; Wang, Y. T.; Ma, X. D., Forecasting
597 PM_{2.5} induced male lung cancer morbidity in China using satellite retrieved PM_{2.5}
598 and spatial analysis. *Sci. Total Environ.* **2017**, *607*, 1009-1017.
- 599 12. Yang, L. W.; Zhang, Y. Z.; Qi, W.; Zhao, T. Y.; Zhang, L. L.; Zhou, L. T.; Ye, L., Adverse
600 effects of PM_{2.5} on cardiovascular diseases. *Reviews on Environmental Health* **2021**.
- 601 13. Kioumourtoglou, M. A.; Schwartz, J. D.; Weisskopf, M. G.; Melly, S. J.; Wang, Y.;
602 Dominici, F.; Zanobetti, A., Long-term PM_{2.5} Exposure and Neurological Hospital

- 603 Admissions in the Northeastern United States. *Environ. Health Perspect.* **2016**, *124*, (1),
604 23-29.
- 605 14. Seiwert, B.; Nihemaiti, M.; Troussier, M.; Weyrauch, S.; Reemtsma, T., Abiotic
606 oxidative transformation of 6-PPD and 6-PPD quinone from tires and occurrence of
607 their products in snow from urban roads and in municipal wastewater. *Water Research*
608 **2022**, *212*.
- 609 15. Wang, W.; Cao, G. D.; Zhang, J.; Chen, Y. Y.; Chen, Z. F.; Qi, Z. H.; Li, R. J.; Dong, C.;
610 Cai, Z. W., Beyond Substituted p-Phenylenediamine Antioxidants: Prevalence of Their
611 Quinone Derivatives in PM2.5. *Environ. Sci. Technol.* **2022**, *56*, (15), 10629-10637.
- 612 16. Zhang, Y.; Xu, C.; Zhang, W.; Qi, Z.; Song, Y.; Zhu, L.; Dong, C.; Chen, J.; Cai, Z., p-
613 Phenylenediamine Antioxidants in PM2.5: The Underestimated Urban Air Pollutants.
614 *Environ. Sci. Technol.* **2021**, *56*, (11), 6914-6921.
- 615 17. Kloeckner, P.; Seiwert, B.; Wagner, S.; Reemtsma, T., Organic Markers of Tire and
616 Road Wear Particles in Sediments and Soils: Transformation Products of Major
617 Antiozonants as Promising Candidates. *Environ. Sci. Technol.* **2021**, *55*, (17), 11723-
618 11732.
- 619 18. Cao, G. D.; Wang, W.; Zhang, J.; Wu, P. F.; Zhao, X. C.; Yang, Z.; Hu, D.; Cai, Z. W.,
620 New Evidence of Rubber-Derived Quinones in Water, Air, and Soil. *Environ. Sci. Technol.*
621 **2022**, *56*, (7), 4142-4150.
- 622 19. Du, B. B.; Liang, B. W.; Li, Y.; Shen, M. J.; Liu, L. Y.; Zeng, L. X., First Report on the
623 Occurrence of N-(1,3-Dimethylbutyl)-N'-phenyl-p-phenylenediamine (6PPD) and
624 6PPD-Quinone as Pervasive Pollutants in Human Urine from South China. *Environ. Sci.*
625 *Technol. Lett.* **2022**, *9*, (12), 1056-1062.
- 626 20. Liang, B. W.; Ge, J. L.; Deng, Q.; Li, Y.; Du, B. B.; Guo, Y.; Zeng, L. X., Occurrence of
627 Multiple Classes of Emerging Synthetic Antioxidants, Including *p*-
628 Phenylenediamines, Diphenylamines, Naphthylamines, Macromolecular Hindered
629 Phenols, and Organophosphites, in Human Milk: Implications for Infant Exposure.
630 *Environ. Sci. Technol. Lett.* **2024**, *11*, (3), 259-265.
- 631 21. Song, S.; Gao, Y.; Feng, S.; Cheng, Z.; Huang, H.; Xue, J.; Zhang, T.; Sun, H.,
632 Widespread occurrence of two typical N, N-substituted p-phenylenediamines and
633 their quinones in humans: Association with oxidative stress and liver damage. *Journal*
634 *of Hazardous Materials* **2024**, *468*.
- 635 22. Fang, J.; Wang, X.; Cao, G.; Wang, F.; Ru, Y.; Wang, B.; Zhang, Y.; Zhang, D.; Yan, J.;
636 Xu, J.; Ji, J.; Ji, F.; Zhou, Y.; Guo, L.; Li, M.; Liu, W.; Cai, X.; Cai, Z., 6PPD-quinone exposure
637 induces neuronal mitochondrial dysfunction to exacerbate Lewy neurites formation
638 induced by α -synuclein preformed fibrils seeding. *Journal of Hazardous Materials* **2024**,
639 *465*.
- 640 23. Tian, Z.; Zhao, H.; Peter, K. T.; Gonzalez, M.; Wetzel, J.; Wu, C.; Hu, X.; Prat, J.;
641 Mudrock, E.; Hettinger, R.; Cortina, A. E.; Biswas, R. G.; Kock, F. V. C.; Soong, R.; Jenne,

642 A.; Du, B.; Hou, F.; He, H.; Lundeen, R.; Gilbreath, A.; Sutton, R.; Scholz, N. L.; Davis, J.
643 W.; Dodd, M. C.; Simpson, A.; McIntyre, J. K.; Kolodziej, E. P., A ubiquitous tire rubber-
644 derived chemical induces acute mortality in coho salmon. *Science* **2021**, *371*, (6525),
645 185-189.

646 24. Wang, W.; Cao, G. D.; Zhang, J.; Chen, Z. F.; Dong, C.; Chen, J. M.; Cai, Z. W., p-
647 Phenylenediamine-Derived Quinones as New Contributors to the Oxidative Potential
648 of Fine Particulate Matter. *Environ. Sci. Technol. Lett.* **2022**, *9*, (9), 712-717.

649 25. Fang, L. Y.; Fang, C. L.; Di, S. S.; Yu, Y. D.; Wang, C. H.; Wang, X. Q.; Jin, Y. X., Oral
650 exposure to tire rubber-derived contaminant 6PPD and 6PPD-quinone induce
651 hepatotoxicity in mice. *Sci. Total Environ.* **2023**, 869.

652 26. Zijin Guo, Z. C., Shaohan Zhang, Hongkai Zhu, Leicheng Zhao, Mujtaba Baqar, Lei
653 Wang, and Hongwen Sun, Unexpected Exposure Risks to Emerging Aromatic Amine
654 Antioxidants and p-Phenylenediamine Quinones to Residents: Evidence from External
655 and Internal Exposure as Well as Hepatotoxicity Evaluation. *Environment & Health*
656 **2024**.

657 27. Kung, H. C.; Uyen, T. P.; Huang, B. W.; Mutuku, J. K.; Chang-Chien, G. P., Evaluation
658 of tire wear particle concentrations in TSP and PM10 using polymeric and molecular
659 markers. *Process Safety and Environmental Protection* **2024**, *184*, 342-354.

660 28. Kumata, H.; Yamada, J.; Masuda, K.; Takada, H.; Sato, Y.; Sakurai, T.; Fujiwara, K.,
661 Benzothiazolamines as tire-derived molecular markers: Sorptive behavior in street
662 runoff and application to source apportioning. *Environmental Science & Technology*
663 **2002**, *36*, (4), 702-708.

664 29. Statistics Bureau of the People's Republic of China. China Statistical Yearbook.
665 *China Statistical Publishing House: Beijing*, 2023.

666 30. Chen, D. Y.; Wang, G. E.; Yuan, Z. W.; Zhang, E. R., Study on the Spatial Pattern and
667 Influencing Factors of China's New Energy Vehicle Industry-Based on Data of Relevant
668 Listed Companies from 2008-2021. *Sustainability* **2023**, *15*, (4).

669 31. Tian, L. L.; Li, J.; Zhao, S. Z.; Tang, J.; Guo, H.; Liu, X.; Zhong, G. C.; Xu, Y.; Lin, T.; Lyv,
670 X. P.; Chen, D. H.; Li, K. C.; Shen, J.; Zhang, G., DDT, Chlordane, and Hexachlorobenzene
671 in the Air of the Pearl River Delta Revisited: A Tale of Source, History, and Monsoon.
672 *Environ. Sci. Technol.* **2021**, *55*, (14), 9740-9749.

673 32. Zhang, R. L.; Zhao, S. Z.; Liu, X.; Tian, L. L.; Mo, Y. Z.; Yi, X.; Liu, S. Y.; Liu, J. Q.; Li, J.;
674 Zhang, G., Aquatic environmental fates and risks of benzotriazoles, benzothiazoles,
675 and p-phenylenediamines in a catchment providing water to a megacity of China.
676 *Environmental Research* **2023**, 216.

677 33. Zhang, R. L.; Zhao, S. Z.; Liu, X.; Thomes., M. W.; Bong, C. W.; D, D. N.; Samaraweera;
678 Priyadarshana, T.; Zhong, G. C.; Li, J.; Zhang, G., Fates of Benzotriazoles, Benzothiazoles,
679 and p-Phenylenediamines in Wastewater Treatment Plants in Malaysia and Sri Lanka.
680 *Environ. Sci. Technol. Water* **2023**, *3*, 1630-1640.

- 681 34. Wang, J. Q.; Jiang, H. Y.; Jiang, H. X.; Mo, Y. Z.; Geng, X. F.; Li, J. B.; Mao, S. D.; Bualert,
682 S.; Ma, S. X.; Li, J.; Zhang, G., Oxidative potential of solvent-extractable organic matter
683 of ambient total suspended particulate in Bangkok, Thailand. *Atmos. Environ.* **2020**, *24*,
684 (3), 400-413.
- 685 35. Geng, X. F.; Zhong, G. C.; Li, J.; Cheng, Z. B.; Mo, Y. Z.; Mao, S. D.; Su, T.; Jiang, H. Y.;
686 Ni, K. W.; Zhang, G., Molecular marker study of aerosols in the northern South China
687 Sea: Impact of atmospheric outflow from the Indo-China Peninsula and South China.
688 *Atmos. Environ.* **2019**, *206*, 225-236.
- 689 36. Harner, T.; Bidleman, T. F., Octanol-air partition coefficient for describing
690 particle/gas partitioning of aromatic compounds in urban air. *Environ. Sci. Technol.*
691 **1998**, *32*, (10), 1494-1502.
- 692 37. Li, Y. F.; Ma, W. L.; Yang, M., Prediction of gas/particle partitioning of
693 polybrominated diphenyl ethers (PBDEs) in global air: A theoretical study. *Atmos.*
694 *Chem. Phys.* **2015**, *15*, (4), 1669-1681.
- 695 38. Li, Y. F.; Qiao, L. N.; Ren, N. Q.; Sverko, E.; Mackay, D.; Macdonald, R. W.,
696 Decabrominated Diphenyl Ethers (BDE-209) in Chinese and Global Air: Levels,
697 Gas/Particle Partitioning, and Long-Range Transport: Is Long-Range Transport of BDE-
698 209 Really Governed by the Movement of Particles? *Environ. Sci. Technol.* **2017**, *51*, (2),
699 1035-1042.
- 700 39. Zhao, S. Z.; Jones, K. C.; Li, J.; Sweetman, A. J.; Liu, X.; Xu, Y.; Wang, Y.; Lin, T.; Mao,
701 S. D.; Li, K. C.; Tang, J.; Zhang, G., Evidence for Major Contributions of Unintentionally
702 Produced PCBs in the Air of China: Implications for the National Source Inventory.
703 *Environ. Sci. Technol.* **2020**, *54*, (4), 2163-2171.
- 704 40. Zajickova, Z.; Parkanyi, C., Photodegradation of 2-mercaptobenzothiazole disulfide
705 and related benzothiazoles. *Journal of Heterocyclic Chemistry* **2008**, *45*, (2), 303-306.
- 706 41. Felis, E.; Sochacki, A.; Magiera, S., Degradation of benzotriazole and benzothiazole
707 in treatment wetlands and by artificial sunlight. *Water Research* **2016**, *104*, 441-448.
- 708 42. Liao, X.; Zou, T.; Chen, M.; Song, Y.; Yang, C.; Qiu, B.; Chen, Z.-F.; Tsang, S. Y.; Qi, Z.;
709 Cai, Z., Contamination profiles and health impact of benzothiazole and its derivatives
710 in PM_{2.5} in typical Chinese cities. *Sci. Total Environ.* **2021**, *17*, (5).
- 711 43. Wagner, S.; Klockner, P.; Reemtsma, T., Aging of tire and road wear particles in
712 terrestrial and freshwater environments-A review on processes, testing, analysis and
713 impact. *Chemosphere* **2022**, 288.
- 714 44. Fishbein, L., Chemicals used in the rubber industry. *Sci. Total Environ.* **1991**, *101*,
715 (1-2), 33-43.
- 716 45. Neumann, M.; Schliebner, I., UBA Texte 127/2019: Protecting the sources of our
717 drinking water - The criteria for identifying persistent, mobile, and toxic (PMT)
718 substances and very persistent, and very mobile (vPvM) substances under EU REACH

719 regulation (EC) No 1907/2006; German Environment Agency (UBA): Dessau-Roßlau,
720 Germany, 2019.

721 46. Li, Z. M.; Kannan, K., Determination of 1,3-Diphenylguanidine, 1,3-Di-o-
722 tolylguanidine, and 1,2,3-Triphenylguanidine in Human Urine Using Liquid
723 Chromatography-Tandem Mass Spectrometry. *Environ. Sci. Technol.* **2023**, *57*, (24),
724 8883-8889.

725 47. Johannessen, C.; Helm, P.; Lashuk, B.; Yargeau, V.; Metcalfe, C. D., The Tire Wear
726 Compounds 6PPD-Quinone and 1,3-Diphenylguanidine in an Urban Watershed.
727 *Archives of Environmental Contamination and Toxicology* **2022**, *82*, (2), 171-179.

728 48. Li, Z. M.; Kannan, K., Occurrence of 1,3-Diphenylguanidine, 1,3-Di-o-tolylguanidine,
729 and 1,2,3-Triphenylguanidine in Indoor Dust from 11 Countries: Implications for
730 Human Exposure. *Environ. Sci. Technol.* **2023**, *57*, (15), 6129-6138.

731 49. Johannessen, C.; Saini, A.; Zhang, X. M.; Harner, T., Air monitoring of tire-derived
732 chemicals in global megacities using passive samplers. *Environmental Pollution* **2022**,
733 314.

734 50. Keri, R. S.; Patil, M. R.; Patil, S. A.; Budagumpi, S., A comprehensive review in
735 current developments of benzothiazole-based molecules in medicinal chemistry.
736 *European Journal of Medicinal Chemistry* **2015**, *89*, 207-251.

737 51. Liu, W. B.; Xue, J. C.; Kannan, K., Occurrence of and exposure to benzothiazoles and
738 benzotriazoles from textiles and infant clothing. *Sci. Total Environ.* **2017**, *592*, 91-96.

739 52. Liu, B.; Xue, D. S.; Tan, Y. M., Deciphering the Manufacturing Production Space in
740 Global City-Regions of Developing Countries-a Case of Pearl River Delta, China.
741 *Sustainability* **2019**, *11*, (23).

742 53. Wan, Y. J.; Xue, J. C.; Kannan, K., Benzothiazoles in indoor air from Albany, New York,
743 USA, and its implications for inhalation exposure. *Journal of Hazardous Materials* **2016**,
744 *311*, 37-42.

745 54. Xue, J. C.; Wan, Y. J.; Kannan, K., Occurrence of benzotriazoles (BTRs) in indoor air
746 from Albany, New York, USA, and its implications for inhalation exposure. *Toxicological*
747 *and Environmental Chemistry* **2017**, *99*, (3), 402-414.

748 55. Liu, X.; Zeng, X.; Dong, G.; Venier, M.; Xie, Q.; Yang, M.; Wu, Q.; Zhao, F.; Chen, D.,
749 Plastic Additives in Ambient Fine Particulate Matter in the Pearl River Delta, China:
750 High-Throughput Characterization and Health Implications. *Environ. Sci. Technol.* **2021**,
751 *55*, (8), 4474-4482.

752 56. Wu, Y.; Venier, M.; Hites, R. A., Broad Exposure of the North American Environment
753 to Phenolic and Amino Antioxidants and to Ultraviolet Filters. *Environ. Sci. Technol.*
754 **2020**, *54*, (15), 9345-9355.

755 57. Burkholder, K. E.; Ludwig, K. N. T., James Robert Composite of Melamine Derivative
756 and Carbon Blank, Rubber Composition and Article Having a Component Thereof. 2003.

757 58. Seiwert, B.; Kloeckner, P.; Wagner, S.; Reemtsma, T., Source-related smart suspect
758 screening in the aqueous environment: search for tire-derived persistent and mobile
759 trace organic contaminants in surface waters. *Analytical and Bioanalytical Chemistry*
760 **2020**, *412*, (20), 4909-4919.

761 59. Niu, F.; Li, Z. Q.; Li, C.; Lee, K. H.; Wang, M. Y., Increase of wintertime fog in China:
762 Potential impacts of weakening of the Eastern Asian monsoon circulation and
763 increasing aerosol loading. *Journal of Geophysical Research-Atmospheres* **2010**, *115*.

764 60. Wang, T.; Li, B.; Zou, X.; Wang, Y.; Li, Y.; Xu, Y.; Mao, L.; Zhang, C.; Yu, W., Emission
765 of primary microplastics in mainland China: Invisible but not negligible. *Water*
766 *Research* **2019**, *162*, 214-224.

767 61. Gossmann, I.; Herzke, D.; Held, A.; Schulz, J.; Nikiforov, V.; Georgi, C.; Evangelidou,
768 N.; Eckhardt, S.; Gerdt, G.; Wurl, O.; Scholz-Böttcher, B. M., Occurrence and
769 backtracking of microplastic mass loads including tire wear particles in northern
770 Atlantic air. *Nature Communications* **2023**, *14*, (1).

771 62. Gao, F. L.; Li, J. X.; Hu, J.; Li, X. G.; Sun, C. J., A Review of Microplastics in China
772 Marine Waters. *Journal of Ocean University of China* **2023**, *22*, (5), 1326-1340.

773 63. Rao, G. Y.; Vejerano, E. P., Partitioning of volatile organic compounds to aerosols: A
774 review. *Chemosphere* **2018**, *212*, 282-296.

775 64. Wu, Y.; Venier, M.; Salamova, A., Spatioseasonal Variations and Partitioning
776 Behavior of Organophosphate Esters in the Great Lakes Atmosphere. *Environmental*
777 *Science & Technology* **2020**, *54*, (9), 5400-5408.

778 65. Li, Y. F.; Ma, W. L.; Yang, M., Prediction of gas/particle partitioning of
779 polybrominated diphenyl ethers (PBDEs) in global air: A theoretical study. *Atmos.*
780 *Chem. Phys.* **2015**, *15*, (4), 1669-1681.

781 66. Okeme, J. O.; Rodgers, T. F. M.; Jantunen, L. M.; Diamond, M. L., Examining the Gas-
782 Particle Partitioning of Organophosphate Esters: How Reliable Are Air Measurements?
783 *Environ. Sci. Technol.* **2018**, *52*, (23), 13834-13844.

784 67. Turpin, B. J.; Huntzicker, J. J.; Hering, S. V., Investigation of organic aerosol sampling
785 artifacts in the Los-Angeles basin. *Atmos. Environ.* **1994**, *28*, (19), 3061-3071.

786 68. Zelenyuk, A.; Imre, D.; Beránek, J.; Abramson, E.; Wilson, J.; Shrivastava, M.,
787 Synergy between Secondary Organic Aerosols and Long-Range Transport of Polycyclic
788 Aromatic Hydrocarbons. *Environ. Sci. Technol.* **2012**, *46*, (22), 12459-12466.

789 69. Perraud, V.; Bruns, E. A.; Ezell, M. J.; Johnson, S. N.; Yu, Y.; Alexander, M. L.; Zelenyuk,
790 A.; Imre, D.; Chang, W. L.; Dabdub, D.; Pankow, J. F.; Finlayson-Pitts, B. J.,
791 Nonequilibrium atmospheric secondary organic aerosol formation and growth.
792 *Proceedings of the National Academy of Sciences of the United States of America* **2012**,
793 *109*, (8), 2836-2841.

- 794 70. Zhao, S. Z.; Tian, L. L.; Zou, Z. H.; Liu, X.; Zhong, G. C.; Mo, Y. Z.; Wang, Y.; Tian, Y. K.;
795 Li, J.; Guo, H.; Zhang, G., Probing Legacy and Alternative Flame Retardants in the Air of
796 Chinese Cities. *Environ. Sci. Technol.* **2021**, *55*, (14), 9450-9459.
- 797 71. Kawamura, K.; Pavuluri, C. M., New Directions: Need for better understanding of
798 plastic waste burning as inferred from high abundance of terephthalic acid in South
799 Asian aerosols. *Atmos. Environ.* **2010**, *44*, (39), 5320-5321.
- 800 72. Simoneit, B. R. T.; Schauer, J. J.; Nolte, C. G.; Oros, D. R.; Elias, V. O.; Fraser, M. P.;
801 Rogge, W. F.; Cass, G. R., Levoglucosan, a tracer for cellulose in biomass burning and
802 atmospheric particles. *Atmos. Environ.* **1999**, *33*, (2), 173-182.
- 803 73. Zhu, C. S.; Cao, J. J.; Tsai, C. J.; Zhang, Z. S.; Tao, J., Biomass burning tracers in rural
804 and urban ultrafine particles in Xi'an, China. *Atmospheric Pollution Research* **2017**, *8*,
805 (4), 614-618.
- 806 74. Yao, X. H.; Chan, C. K.; Fang, M.; Cadle, S.; Chan, T.; Mulawa, P.; He, K. B.; Ye, B. M.,
807 The water-soluble ionic composition of PM_{2.5} in Shanghai and Beijing, China. *Atmos.*
808 *Environ.* **2002**, *36*, (26), 4223-4234.
- 809 75. Marr, L. C.; Kirchstetter, T. W.; Harley, R. A.; Miguel, A. H.; Hering, S. V.; Hammond,
810 S. K., Characterization of polycyclic aromatic hydrocarbons in motor vehicle fuels and
811 exhaust emissions. *Environ. Sci. Technol.* **1999**, *33*, (18), 3091-3099.
- 812 76. Streets, D. G.; Bond, T. C.; Carmichael, G. R.; Fernandes, S. D.; Fu, Q.; He, D.; Klimont,
813 Z.; Nelson, S. M.; Tsai, N. Y.; Wang, M. Q.; Woo, J. H.; Yarber, K. F., An inventory of
814 gaseous and primary aerosol emissions in Asia in the year 2000. *Journal of Geophysical*
815 *Research-Atmospheres* **2003**, *108*, (D21).
- 816 77. Ho, K. F.; Zhang, R. J.; Lee, S. C.; Ho, S. S. H.; Liu, S. X.; Fung, K.; Cao, J. J.; Shen, Z.
817 X.; Xu, H. M., Characteristics of carbonate carbon in PM_{2.5} in a typical semi-arid area
818 of Northeastern China. *Atmos. Environ.* **2011**, *45*, (6), 1268-1274.
- 819 78. Matthaios, V. N.; Lawrence, J.; Martins, M. A. G.; Ferguson, S. T.; Wolfson, J. M.;
820 Harrison, R. M.; Koutrakis, P., Quantifying factors affecting contributions of roadway
821 exhaust and non-exhaust emissions to ambient PM_{10-2.5} and PM_{2.5-0.2} particles. *Sci.*
822 *Total Environ.* **2022**, 835.
- 823 79. Contini, D.; Genga, A.; Cesari, D.; Siciliano, M.; Donato, A.; Bove, M. C.; Guascito,
824 M. R., Characterisation and source apportionment of PM₁₀ in an urban background
825 site in Lecce. *Atmospheric Research* **2010**, *95*, (1), 40-54.
- 826 80. Yin, G. C.; Zhu, H. H.; Chen, Z. L.; Su, C. H.; He, Z. C.; Chen, X. L.; Qiu, J. R.; Wang, T.
827 Y., Spatial Distribution and Source Apportionment of Soil Heavy Metals in Pearl River
828 Delta, China. *Sustainability* **2021**, *13*, (17).
- 829 81. Pan, S.; Sun, Y.; Zhang, G.; Li, J.; Xie, Q.; Chaktaborty, P., Assessment of 2-(4-
830 morpholinyl) benzothiazole (24MoBT) and N-cyclohexyl-2-benzothiazolamine (NCBA)
831 as traffic tracers in metropolitan cities of China and India. *Atmos. Environ.* **2012**, *56*,
832 246-249.

833 82. Rodland, E. S.; Gustafsson, M.; Jaramillo-Vogel, D.; Järnskog, I.; Müller, K.; Rauert,
834 C.; Rausch, J.; Wagner, S., Analytical challenges and possibilities for the quantification
835 of tire- road wear particles. *Trac-Trends in Analytical Chemistry* **2023**, 165.

836 83. Xiong, Q. L.; Zhao, W. J.; Guo, X. Y.; Shu, T. T.; Chen, F. T.; Zheng, X. X.; Gong, Z. N.,
837 Dustfall Heavy Metal Pollution During Winter in North China. *Bulletin of Environmental*
838 *Contamination and Toxicology* **2015**, 95, (4), 548-554.

839 84. Weyrauch, S.; Seiwert, B.; Voll, M.; Wagner, S.; Reemtsma, T., Accelerated aging of
840 tire and road wear particles by elevated temperature, artificial sunlight and
841 mechanical stress - A laboratory study on particle properties, extractables and
842 leachables. *Sci. Total Environ.* **2023**, 904.

843 85. Yang, K.; Chen, D. H.; Ding, X.; Li, J.; Zhang, Y. Q.; Zhang, T.; Wang, Q. Y.; Wang, J. Q.;
844 Cheng, Q.; Jiang, H.; Liu, P.; Wang, Z. R.; He, Y. F.; Zhang, G.; Wang, X. M., Different roles
845 of primary and secondary sources in reducing PM_{2.5}: Insights from molecular markers
846 in Pearl River Delta, South China. *Atmos. Environ.* **2023**, 294.

847 86. Huang, X. F.; Zou, B. B.; He, L. Y.; Hu, M.; Prévôt, A. S. H.; Zhang, Y. H., Exploration
848 of PM_{2.5} sources on the regional scale in the Pearl River Delta based on ME-2 modeling.
849 *Atmos. Chem. Phys.* **2018**, 18, (16), 11563-11580.

850 87. Timmers, V.; Achten, P. A. J., Non-exhaust PM emissions from electric vehicles.
851 *Atmos. Environ.* **2016**, 134, 10-17.

852 88. Cao, L.; Deng, F.; Zhuo, C. F.; Jiang, Y. Y.; Li, Z. B.; Xu, H. C., Spatial distribution
853 patterns and influencing factors of China's new energy vehicle industry. *Journal of*
854 *Cleaner Production* **2022**, 379.

855 89. Su, C. W.; Yuan, X.; Shao, X. F.; Moldovan, N. C., Explore the environmental benefits
856 of new energy vehicles: evidence from China. *Annals of Operations Research* **2023**.

857